Measurement of the Wigner function of an ensemble of helium atoms

Ch. Kurtsiefer, T. Pfau & J. Mlynek

Fakultät für Physik, Universität Konstanz, Postfach 5560, D-78434 Konstanz, Germany

Beams of atoms can exhibit interference and diffraction phenomena just like waves of light. For a coherent beam of helium atoms in a double-slit experiment, measurements of the quantum-mechanical analogue of the classical phase-space distribution function show that the motion of atoms behaves in a strongly non-classical manner.

Over the past few years, techniques for manipulating the motion of atoms using light fields or micro-structured solids have undergone rapid development[1], and they now provide the fundamental tools for the new field of 'atom optics'. Underlying these techniques is the insight of de Broglie that a particle of mass m moving with a velocity v can be viewed as a matter wave with wavelength $\lambda_{dB} = 2\pi\hbar/(mv)$. Based on this wave nature, atom interferometers have been demonstrated[2,3], which are now finding applications in precision spectroscopy and atomic physics[4].

Most of the atom interferometers realized to date rely on the fact that the quantum-mechanical state of motion that describes the atoms is such that, at some point in the experiment, they are in a superposition state of being at two different locations x in space, which may be micrometres to centimetres apart. The matter wavefunction corresponding to such a state cannot, however, be measured for a single atom, and the measurement has to be performed on an ensemble of similarly prepared atoms. The full quantum-mechanical description of an ensemble system needs to capture both intrinsic quantum-mechanical uncertainties and possible uncertainties due to a 'classical' lack of knowledge about the initial exact quantum state of each particle in the ensemble. The most complete descriptions are provided by the Wigner function $W(x, p)$ (where p is momentum) which was introduced as early as 1932 (ref. 5) or alternatively the density matrix $\hat{\rho}(x, x')$. These two quantities are related by

$$W(x, p) = \frac{1}{\pi\hbar}\int \langle x + x' \mid \hat{\rho} \mid x - x' \rangle e^{i2px'/\hbar} dx'$$

The Wigner function offers a convenient interpretation of the ensemble in the form of a quasi-probability distribution in the phase space defined by position x and momentum p. For quasi-classical states of a system, $W(x, p)$ is identical to the phase-space density of the corresponding classical system[6]. There are, however, states of systems which do not have a classical equivalent at all, such as that of a particle in an atom interferometer when in a linear superposition of states at two spatially separated locations. These states lead to negative values in the quasi-probability distribution $W(x, p)$; in fact, most non-classical states of systems (except those whose variables are described by a gaussian probability distribution) should show negative values in $W(x, p)$. A review of Wigner functions in quantum mechanics can be found in, for example, ref. 7.

It was pointed out by Bertrand and Bertrand[8] and independently by Vogel and Risken[9] that the Wigner function of a system can be reconstructed by tomographical methods from the measured distributions of observables that are certain combinations of the non-commuting variables forming the phase space. Additionally, more sophisticated methods have been developed for the reconstruction of the density matrix as an equivalent complete description of a quantum state[10–12].

There have been several experimental measurements of Wigner functions performed for non-classical states of light[13,14], as well as measurements of the equivalent function that describes molecular vibrational states[15]. Compared to quantum-mechanical states of the electromagnetic field, it is relatively easy to generate a quantum state for a massive particle, such that the wavefunction is a coherent superposition of being at one of two places in space. Very recently, there have been investigations of the state of motion of ions in a harmonic potential by the group of D. Wineland at NIST in Boulder[16], where negativities in the Wigner functions corresponding to Fock states were observed[17]. We investigate here the conceptually simple system of a two-peaked matter wave state prepared by coherent illumination of a double slit, where the state of the particle after preparation is governed by free evolution through the apparatus. When the spatially separated wave packets corresponding to each slit show sufficient mutual coherence, the Wigner function shows negative parts. A detailed theoretical analysis of such a system is given by Janicke and Wilkens[18].

Theoretical background

Phase-space tomography requires a set of measured projections of the Wigner function $W(x, p)$ along different directions in phase space. To avoid the problem of mixing the different physical properties of the conjugated variables x and p for the projection along oblique phase-space directions, we introduce a scaling length x_0 and momentum $p_0 = \hbar/x_0$. A rotated basis ($x' = \tilde{x}\cos\Theta + \tilde{p}\sin\Theta$; $p' = -\tilde{x}\sin\Theta + \tilde{p}\cos\Theta$) for the phase space can then be expressed by a reduced position $\tilde{x} = x/x_0$ and momentum $\tilde{p} = p/p_0$, and a mixing angle Θ. The projections or marginal distributions of a motional state described by the Wigner function $W_0(\tilde{x}, \tilde{p})$ are then given by

$$P_\Theta(x') = \int dp' W_0(\tilde{x}, \tilde{p})$$

After a motional state $W_0(\tilde{x}, \tilde{p})$ is prepared, a physical mixing mechanism between x and p has to be introduced to measure the marginal distributions in a set of observables $x'(\Theta)$. This mixing mechanism can be provided by a combination of lenses and free-space propagation for arbitrary complex-valued fields[19–21]; the key idea is to change a momentum distribution (or a distribution in a mixed base) into a position distribution $P(x)$, which then can be observed with an atom detector. The simplest mixing mechanism is the free evolution of the particle, using the kinetic-energy hamiltonian $H = p^2/2m$. Under this hamiltonian, the Wigner function W_0

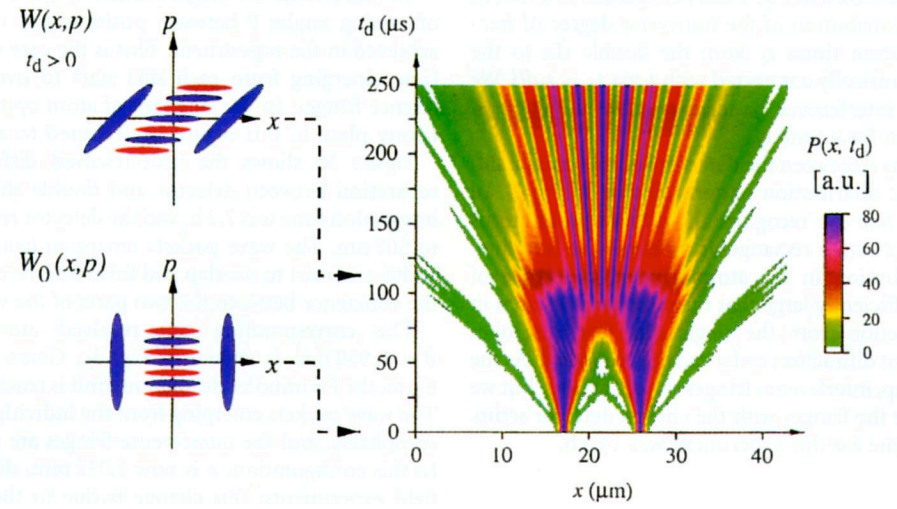

Figure 1 Evolution of a quantum state W_0 initially in a superposition of an atom being behind one of two slits. The two large blue vertical ellipses illustrate the position–momentum (x–p) distribution of atoms isolated behind one or other of the slits (the quasi-classical states); the alternating blue and red horizontal ellipses illustrate the position–momentum distribution of the atoms in the non-classical superposition of states (red corresponds to negative values in the Wigner function)–it is these superposition states that give rise to interference. After an evolution time t_d, the Wigner function becomes sheared in phase space, and in the corresponding position distribution (main figure) $P(x,t_d)$, interference fringes appear. The plot was obtained by numerical evaluation using Huygens–Fresnel diffraction, where the double slit is illuminated from an incoherent matter wave source with a finite spatial extent of 5 μm, corresponding to our experimental situation (a.u., arbitrary units).

of the initial state is sheared in phase space (Fig. 1). This can be easily understood from the classical equation of motion $\partial x/\partial t = p/m$ for a point in phase space. The position distributions from the sheared Wigner function for a set of evolution times t_d may contain enough information to approximately reconstruct the original Wigner function[20], as is the case for a set of marginal distributions $P_\Theta(x')$. In fact, a huge class of hamiltonians can be used to modify a given state W_0 such that its initially hidden aspects can be revealed by only measuring its position distribution after a set of evolution times[22,23]. Free evolution seems to be just the simplest choice in the case of a massive particle.

Experimental realization

The experimental apparatus is shown in Fig. 2. A beam of metastable helium atoms is generated in a gas-discharge source, which is used in a pulsed operation mode by switching the discharge current. A fraction of the atoms in the beam are in the metastable 2^3S_1 state, produced by electron impact during the switch-on time of 15 μs. The longitudinal velocity distribution of the metastable atom beam emerging from the source consists of a fraction of very fast atoms with velocity $v \approx 33{,}000\ \mathrm{m\,s^{-1}}$ and a fraction at velocities between 1,000 and 3,000 $\mathrm{m\,s^{-1}}$ corresponding to the thermal energy of the helium gas expanding in a nozzle. The beam passes a skimmer and is collimated by a 5-μm-wide slit. Further downstream, the beam is sent through a micro-fabricated double-slit structure with a slit separation of 8 μm and an opening of 1 μm. The experiments are conducted under high vacuum conditions (10^{-6} mbar). The combination of entrance slit and double slit acts as a preparation tool for the transverse motion of the atoms. The atoms then propagate for a distance d to a time- and space-resolving detector[24]; this detector is based on the fact that metastable (that is, electronically excited) atoms release secondary electrons when striking a metal surface[25]. Our detector allows us to measure the transverse atomic distribution of metastable atoms with a spatial resolution down to 500 nm, and the arrival time t_f (after leaving the source) of the atoms with an accuracy of 100 ns. From an atom-optical point of view, this corresponds to measurements of atomic distributions corresponding to different de Broglie wavelengths $\lambda_{dB} = 2\pi\hbar/(mv)$, where m is the mass of a He atom and $v = l/t_f$ (l is the source-detector distance). The mean number of detected atoms per source pulse varies from 0.01 to 0.2; the source is repeatedly fired, and the obtained distribution summed up.

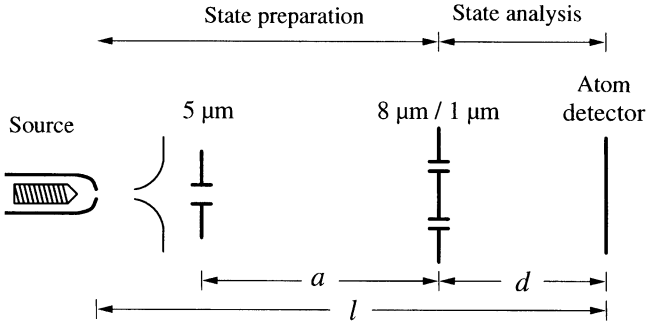

Figure 2 Diagram of apparatus used to observe atomic interference patterns. The single slit is 5 μm wide; the double slit has a slit separation of 8 μm and a slit width of 1 μm. The experiment is conducted under high vacuum conditions. See text for details.

For the very fast atoms, the wave packet associated with the transverse motion has not enough time to spread out in space, so the transverse distribution of the atom stays as prepared by the double-slit structure. In the language of atom optics, this may be regarded as a geometrical shadow of the structure on the detector. Because the double slit is illuminated from a single slit rather than a source emitting a plane matter wave, the observed shadow is magnified by a factor $(a + d)/a$, where a is the distance between the single slit and the double slit. In the experiment, we use this information to gauge the length scaling of the detector.

Time-resolved diffraction patterns

Because the longitudinal motion of the atoms at velocities v of several thousand metres per second may be treated completely

classically, the apparatus shown in Fig. 2 can be regarded as a tool to investigate the spatial distribution of the transverse degree of freedom for a set of evolution times t_d from the double slit to the detector, which is geometrically connected with t_f via $t_d = t_f d/l$. We therefore describe the interference patterns that we obtained in terms of a free evolution for a time t_d.

For a set of separations d between the detector and the double slit, we obtained the atomic distribution patterns shown in Fig. 3. In Fig. 3a ($d = 148$ mm), one can recognize the diffraction of atoms from the individual slits with a rectangular transmission function. For the velocity distribution in the atomic beam, the range of evolution times t_d is sufficiently large that the detector is located in the far field for diffraction from the single slits; the side lobes corresponding to the first diffraction order can be recognized. As the two wave packets overlap, interference fringes should appear, but we were not able to resolve the fringes with the chosen detector setup. The total integration time for this experiment was 14.5 h.

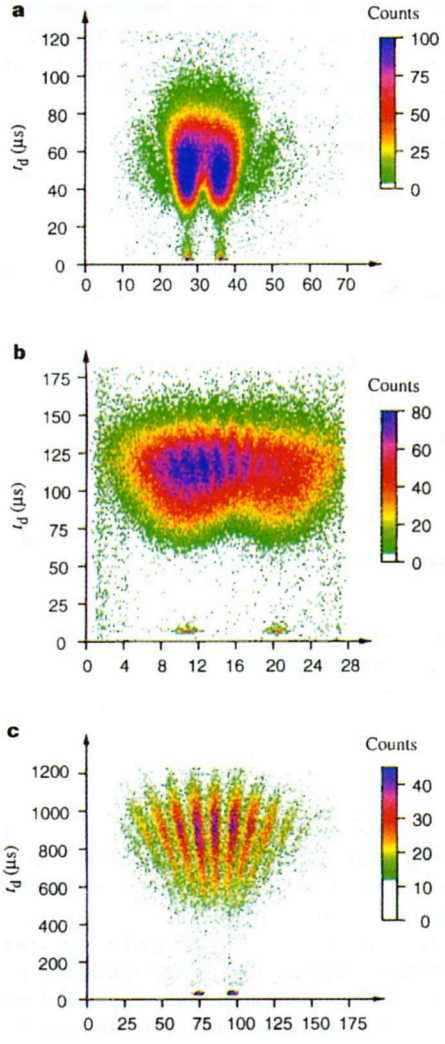

Figure 3 Distribution of atoms in the detection plane as a function of their velocities. This corresponds to different evolution times for a partial coherent matter wave packet after the double slit. **a**, For a separation $d = 148$ mm between detector and double slit (see Fig. 2). The diffraction pattern is determined by the diffraction from the single slits. **b**, For the transition regime at $d = 248$ mm. Partial waves from both slits start to interfere. **c**, For a separation $d = 1{,}950$ mm (far field). The interference orders are clearly separated, and their separation grows linearly with the evolution time.

To reconstruct the Wigner function W_0, a sufficiently large range of mixing angles θ between position and momentum has to be achieved in the experiment. This is the case when the two wavelets (one emerging from each slit) start to overlap and form interference fringes. In the language of atom optics, interference effects taking place in this regime are referred to as Fresnel diffraction.

Figure 3b shows the time-resolved diffraction pattern for a separation between detector and double slit of $d = 248$ mm; the integration time was 7.2 h, and the detector resolution was increased to 500 nm. The wave packets emerging from each slit increase in width and start to overlap and form interference fringes, indicating the coherence between the two parts of the wavefunction.

The corresponding time-resolved atomic distribution for $d = 1{,}950$ mm is shown in Fig. 3c. Given the slit separation of 8 μm, the Fraunhofer diffraction limit is reached for the slow atoms. The wave packets emerging from the individual slits overlap almost completely, and the interference fringes are most clearly observed. In this configuration, a is now 1,052 mm, differing from the near-field experiments; this change is due to the requirements of the apparatus. To compensate for the small atom flux seen by the detector because of its large separation from the source, we had to extend the integration time in this experiment to 49 h.

Reconstruction of the Wigner function

The transformation algorithm used to reconstruct the prepared Wigner function is similar to that described in ref. 18. Free evolution of the particle for a time t_d leads to a corresponding position distribution $P(\tilde{x}, t_d)$, which is connected with a rotated marginal

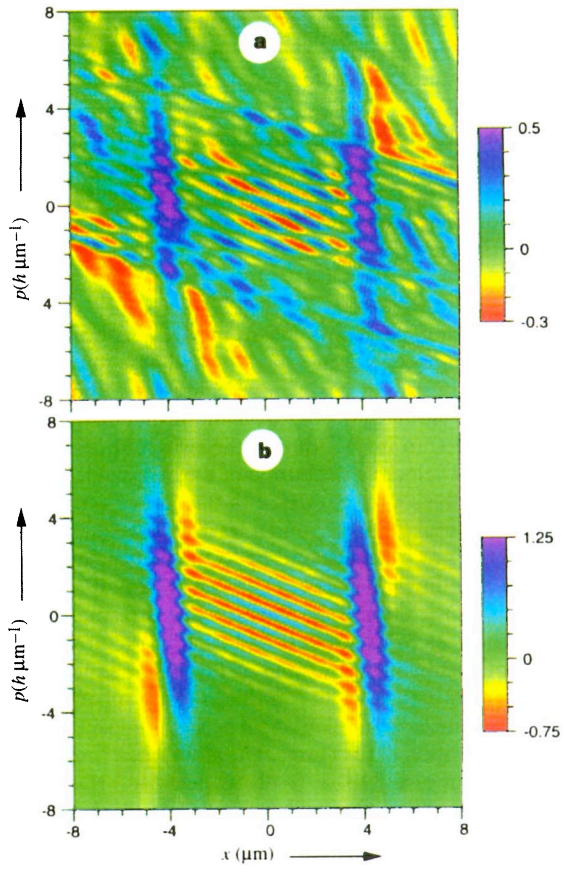

Figure 4 **a**, Reconstructed Wigner function $W(x,p)$ of the investigated atomic ensemble, obtained from the experimental distribution shown in Fig. 3b using the inverse Radon transformation[13,18]. **b**, Reconstruction of $W(x,p)$ from the numerical distribution in Fig. 1.

distribution $P_\Theta(\tilde{x})$ by:

$$P_\Theta(\tilde{x}) = P\left(\frac{\tilde{x}}{\cos\Theta}, \frac{mx_0^2}{\hbar}\tan\Theta\right)$$

As there is only access to positive evolution times t_d, free evolution only gives access to rotated marginal distributions P_Θ for angles Θ between 0 and $\pi/2$. Theoretical investigations[18,19] have shown that the use of additional optical elements (lenses) could allow the complete set of mixing angles Θ ($-\pi/2$ to $\pi/2$) to be investigated; this is necessary to reconstruct a completely unknown state. Alternatively, additional symmetry assumptions can be made for the Wigner function investigated, such as left/right symmetry or time-reversal symmetry. Here we use assumption of symmetry in position space for the reconstructed Wigner function.

Furthermore, only a limited range of evolution times t_d is available in an experiment. But by choosing an appropriate range of evolution times, the interesting information of a system should be contained in the observed distributions. Here, the information is the coherence property of two spatially separated wave packets.

Another problem for the reconstruction process is the coupling between longitudinal and transverse motion, as we illuminate the double slit from a single slit instead of a pure plane-wave source. This effect can be taken into account by rescaling the transverse position in the detection plane by the factor $a/(a+d)$ of geometrical magnification; the evolution-time-dependent mixing process between position and momentum is preserved.

The reconstructed Wigner function we obtained from the diffraction data shown in Fig. 3b is shown in Fig. 4a, where we chose a scaling length $x_0 = 2\,\mu$m and a cut-off frequency $r_c = 10$ (see ref. 18 for details). The two positive regions, corresponding to the spatial distribution of the atoms during preparation, may be seen. The separation between the regions ($\sim 8\,\mu$m) corresponds to the position distribution in the plane of the double slit; the information relevant to determining this feature of the Wigner function is mainly contributed by the very fast atoms. The coherence between the two spatially separated parts of the Schrödinger field at the position of the double slit then leads to interference, which is manifested in oscillations in the Wigner function in the region between the two main 'blobs'. In this region, the reconstructed Wigner function takes negative values, indicating a property which cannot be obtained by classical phase-space distributions and revealing the quantum nature of the observed ensemble of atoms.

But, in contrast to what is expected[18], the reconstructed Wigner function appears sheared, and regions of negative value appear close to the two large positive blobs. This is consistent with the reconstruction shown in Fig. 4b which was obtained from the numerically obtained distributions shown in Fig. 1, where the largest evolution time was restricted to 175 μs; the shear and the regions of negative value close to the positive blobs are therefore a consequence of the reconstruction algorithm. The non-physical shear disappears if longer evolution times t_d for the observed marginal distributions $P(x, t_d)$ are allowed, as additional numerical tests have shown.

More sophisticated reconstruction techniques than the inverse Radon transform[13,18] could therefore be usefully applied to our data. Promising tools for reconstructing the Wigner function from such an incomplete set of measured marginal distributions may be a technique using bayesian analysis (described in ref. 11 for application in optical homodyne tomography) or maximum entropy algorithms (as suggested by V. Bužek *et al.*[12]).

Here we have reported on the measurement of the Wigner function of a massive particle wave packet formed by partially coherent illumination of a double slit; we have been able to identify negative parts in the oscillatory part of the Wigner function corresponding to a superposition of macroscopically separated parts of the matter wave field. In quantum optics, such a state is sometimes referred to as a 'Schrödinger cat state'[16].

Our technique provides a convenient approach to detection of particles for which the key observables, position and momentum, can be mixed controllably. Such a choice of a detection base would be necessary for Bell-type experiments[26] with entangled atom–photon pairs, which can be efficiently produced and detected[27]. The measurement technique reported here could be used for measuring the atomic part of these pairs. It may also be useful in characterizing the motional state of atoms emerging from one of the new atomic sources currently under discussion in the context of Bose condensates. □

Received 4 November 1996; accepted 21 January 1997.

1. Adams, C. S., Sigel, M. & Mlynek, J. *Phys. Rep.* **240,** 143–210 (1994).
2. Carnal, O. & Mlynek, J. *Phys. Rev. Lett.* **66,** 2689–2692 (1991).
3. Keith, D. W., Ekstrom, C. R., Turchette, Q. A. & Pritchard, D. E. *Phys. Rev. Lett.* **66,** 2693–2696 (1991).
4. Berman, P. (ed.) *Atom Interferometry* (Academic, San Diego, 1997).
5. Wigner, E. *Phys. Rev.* **40,** 749–759 (1932).
6. Royer, A. *Foundat. Phys.* **19,** 3–32 (1989).
7. Hillery, M., O'Conell, R. F., Scully, M. O. & Wigner, E. P. *Phys. Rep.* **106,** 121–167 (1984).
8. Bertrand, J. & Bertrand, P. *Foundat. Phys.* **17,** 397–405 (1987).
9. Vogel, K. & Risken, H. *Phys. Rev. A* **40,** 2847–2849 (1989).
10. D'Ariano, G. M., Macciavello, C. & Paris, M. G. A. *Phys. Rev. A* **50,** 4298–4302 (1994).
11. Tan, S. M. *J. Mod. Opt.* (submitted).
12. Buszek, V., Adam, G. & Drobný, G. *Ann. Phys.* (NY) **254,** 37–97 (1996).
13. Smithey, D. T., Beck, M., Raymer, M. G. & Faridani, A. *Phys. Rev. Lett.* **70,** 1244–1247 (1993).
14. Breitenbach, G. *et al. J. Opt. Soc. Am. B* **12,** 2304–2309 (1995).
15. Dunn, T. J., Walmsley, I. A. & Mukamel, S. *Phys. Rev. Lett.* **74,** 884–887 (1995).
16. Monroe, C., Meekhof, D. M., King, B. E. & Wineland, D. J. *Science* **272,** 1131–1135 (1996).
17. Leibfried, D., King, B. E., Monroe, C., Itano, M. & Wineland, D. J. *Phys. Rev. Lett.* **77,** 4281–4285 (1996).
18. Janicke, U. & Wilkens, M. *J. Mod. Opt.* **42,** 2183–2199 (1995).
19. Raymer, M. G., Beck, M. & McAlister, D. F. *Phys. Rev. Lett.* **72,** 1137–1140 (1994).
20. Lohmann, A. W. *J. Opt. Soc. Am. A* **10,** 2181–2186 (1993).
21. Kienle, S. H., Freyberger, M., Schleich, W. P. & Raymer, M. G. in *Experimental Metaphysics: Quantum Mechanical Studies for Abner Shimony* (eds Cohen, R. S., Horne, M. A. & Stachel, J.) 121–133 (Kluwer, Dordrecht, 1997).
22. Richter, Th. & Wünsche, A. *Phys. Rev. A* **53,** 1974–1977 (1996).
23. Leonhard, U. & Raymer, M. G. *Phys. Rev. Lett.* **76,** 1985–1989 (1996).
24. Kurtsiefer, Ch. & Mlynek, J. *Appl. Phys. B* **64,** 85–90 (1996).
25. Hotop, H. in *Methods of Experimental Physics* Vol. 29B (eds Dunning, F. B. & Hulet, R. G.) 191–215 (Academic, San Diego, 1995).
26. Pfau, T., Kurtsiefer, Ch. & Mlynek, J. *Quant. Semiclass. Opt.* **8,** 665–671 (1996).
27. Kurtsiefer, Ch. *et al. Phys. Rev. A* (submitted).

Acknowledgements. We thank U. Janicke and M. Wilkens for discussions. This work was supported by the Deutsche Forschungsgemeinschaft.

Correspondence and requests for materials should be addressed to Ch.K. (e-mail: christian.kurtsiefer@uni-konstanz.de).